RSC Advances

PAPER

View Article Online
View Journal | View Issue

Cite this: *RSC Adv.*, 2023, **13**, 2355

Investigating the photosensitization activities of flavins irradiated by blue LEDs†

Jonathan Ribes, Pauline Cossard, Khaled Al Yaman, Isabelle Bestel and Eduard Badarau *

Received 20th November 2022
Accepted 5th January 2023

DOI: 10.1039/d2ra07379j

rsc.li/rsc-advances

Due to their ability to easily absorb light and to generate highly reactive species, photosensitizers emerged as promising tools in a wide variety of physico-chemical and biological processes. Natural photosensitizers have the benefit of a life-compatible toxicological profile. Porphyrins and flavins are such examples that already proved their efficiency as photo-dynamic therapeutics. The present article describes a reliable, easy-to-implement, readily available and reproducible method that can be used to characterize the photosensitizing activity of flavins. Several key factors were investigated during this study, the optimum parameters were: (i) a blue LED light source (λ_{em} = 455 nm) at 6.69 mW; (ii) a pH of 6 mimicking the tumoral environment; (iii) an air-saturated atmosphere reaction medium, (iv) a tetrazolium dye (MTT) was used to monitor the photosensitization efficacy *via* the generation of the colored MTT-formazan product. This method can be used to rank a series of flavins based on their photosensitizing activities. Such structure–photosensitization activity relationships are essential for the discovery of future potent photosensitizers for photodynamic therapy.

Introduction

Photosensitizers are molecular systems able to efficiently generate an excited state by absorbing light (photons).[1] Contrarily to other molecules, the excited photosensitizer has a lifetime (τ) long enough to allow it to react with its neighboring environment, before returning to its original ground-state. The ability of a photosensitizer to easily absorb light is intimately related to its molecular structure: in the case of organic materials, a highly conjugated π-system is essential to promote photoexcitation.[2] While the photo-dynamic therapy (PDT) is by far the most well-known and studied application of photosensitizers,[3–5] other utilizations are also described in the literature, for example: as catalysts in synthesis[6] or pollutants degradations,[7] as initiators in crosslinking or degradation of polymers,[8] as key elements for the construction of solar energy conversion systems[9,10] or as chromophores for optical power limiting systems.[7]

Among the small-molecule photosensitizers, natural photosensitizers have already proved their efficiency, as they are currently used in clinics: porphyrins and flavins are such examples. In its native environment, riboflavin (RF, vitamin B2) and its metabolically active derivatives (flavin mononucleotide – FMN and flavin adenine dinucleotide – FAD) are involved in light-activated physiological processes.[11] Activated by the blue light (λ = 445 nm), RF is used in clinics for treating keratoconus[12,13] or for sterilizing blood components.[14–16]

Natural photosensitizers cannot be used in their native state in many applications, and require specific modulations in order to either conjugate them on a material or to modify their physico-chemical properties.[17–19] As these structural modifications can impact their photosensitizing properties, it is often necessary to reassess the photosensitizer's activity through a reliable evaluation method of the induced photosensitizing reactions.

The efficiency of flavins as photosensitizers is highly dependent on their ability to promote photosensitizing reactions. In the case of flavins, the most studied photosensitizing reactions are: (a) type I reactions where the activated photosensitizer reacts directly with a substrate and (b) type II reactions, where singlet oxygen ($^1O_2$), a highly reactive oxygenated species (ROS), is firstly generated by the activated photosensitizer, followed by the reaction of the $^1O_2$ with a substrate (Fig. 1A).[20,21] Depending on the lifetime and the concentrations of the excited species (substrate or oxygen), one or the other pathway will be favored, but in general they co-exist. Compared to the lifetime of singlet oxygen in water (evaluated at 3 µs), in the case of flavins, their lifetime is substantially longer (for example, for triplet RF, ^{3}RF*, τ = 15 µs).[22] It should also be

University of Bordeaux, CNRS, CBMN, UMR 5248, Institute of Chemistry and Biology of Membranes & Nano-objects (CBMN), Allée Geoffroy Saint Hilaire, Bât B14, 33600 Pessac, France. E-mail: edouard.badarau@u-bordeaux.fr

† Electronic supplementary information (ESI) available: Calibration curve for MTT-formazan used to calculate the photosensitizing activity of flavins, the pH dependence of the absorbance for the MTT formazan, the control reactions in the absence of methionine and of riboflavin, as well as the ^{1}H- and ^{13}C-NMR spectra of the newly synthesized compounds. See DOI: https://doi.org/10.1039/d2ra07379j

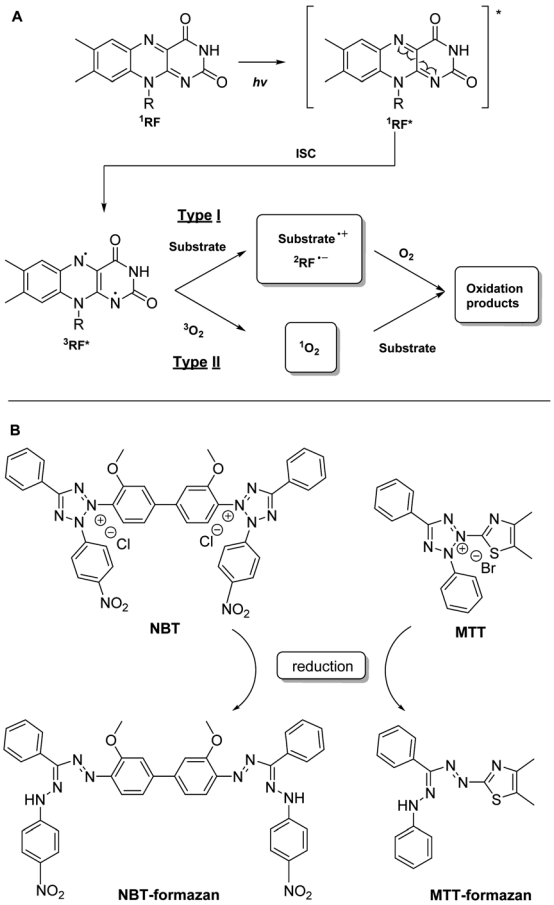

Fig. 1 (A) Main photosensitizing reactions pathways described for riboflavin: (a) type I involves direct reaction of the excited photosensitizer with the substrate and (b) type II involves substrate modification by singlet oxygen ($^1O_2$) generated by the excited photosensitizer;[26,27] (B) chemical structures of NBT and MTT dyes and their reduced forms.

mentioned that flavoenzymes can stabilize excited flavins through geometrical and electrostatic interactions, compared to the non-bound flavins.[23]

Although complex and focused mainly on a fundamental understanding of the physico-chemical process driving the radical reactions, studies that characterize individually the type I or the type II reactions do exist[24–26] and are conducted on simplified model systems. We were interested in the development of a method able to characterize the photosensitizing activity of a sensitizer in a complex biological environment. Consequently, our interest was not in discriminating the type I from the type II reactions, but on the global output, thus summing up both pathways. We intended to develop a reliable and easy-to-implement protocol that can be used to conduct structure–photosensitizing activity relationships (SAR) on flavins. This protocol is essential during medicinal chemistry projects, when a series of flavin analogues are synthesized with the goal of identifying new potent photosensitizers: they should be ranked based on their photosensitizing activities, ideally using a flavin reference during the same study (riboflavin, FMN or FAD, being the most commonly used flavin standards).

An important criterion for our study was the use of *in vivo*-compatible conditions: an aqueous reaction environment, a pH range and an atmosphere specific to the targeted biological environment, reagents that are non-toxic (or having an acceptable toxicity profile already approved by other cell studies) and a life-compatible source of light.

Several methods are described in the literature for the characterization of the photosensitizing activity. They are focused on either the direct monitoring of the generated ROS[28] or indirectly by monitoring the behavior of a probe.[28,29] Among them, the colorimetric methods are easy to implement and to adapt to different biological systems. Briefly, a colored indicator will modify its absorbance when reacted with a photosensitizer. Monitoring the hyper/hypsochromic effect of the indicator will thus reveal the photosensitizer's activity.

One such colorimetric test was described for flavins by Liang *et al.*:[30] it involves the use of riboflavin as photosensitizer and nitro-blue-tetrazolium (NBT) as indicator (Fig. 1B). The riboflavin is excited by a blue LED to the excited singlet state, subsequently generating ^{3}RF*, which is reduced to a semiquinone state by methionine. RF semiquinone can reduce NBT, either in ground or in an excited state, to the corresponding formazan (directly *via* a type I reaction or indirectly *via* a type II reaction). As the generated formazan is absorbing at 560 nm, its concentration can be directly correlated with the activity of the photosensitizer.

We reproduced this test for riboflavin, but in our hands this protocol was difficult to master. Thus, we started a methodological approach to identify, and eventually optimize, the key parameters governing this reaction.

Results and discussion

Starting from the method previously reported by Liang *et al.*[30] and summarized above, several parameters were investigated during our study: the choice of the indicator, the concentration of the sensitizer, the influence of the irradiation source, the influence of the pH, as well as that of the reaction's atmosphere. These will be detailed in the following sections.

1 Design of the blue LED-promoted photosensitization-reaction

a Choice of the tetrazolium indicator. One of the main issues of the colorimetric tests concerns the aqueous solubility of the dye. Despite the possible ionization state of the colorant molecule (*e.g.* salt) enhancing its hydrophilicity, a highly conjugated system necessary to induce an absorption in the visible range boosts its lipophilicity. The partition coefficient ($\log P$) of the dye is thus a key parameter to take into account when monitoring the dye's concentration using the Beer–Lambert law.

We started our study using an NBT indicator, as previously described in the literature for monitoring riboflavin photosensitizing activity.[30] Unfortunately, after reaction with the light-activated riboflavin, the reduced NTB (NBT-formazan) is only partly soluble in water. For example, an important

sedimentation of the formed NBT formazan is observed if the reaction mixture is immobilized for 20 min: the absorbance decreased by half compared to the one recorded immediately after the reaction. This was clearly shown by passing the reaction mixture on a polytetrafluoroethylene (PTFE) syringe filter (0.2 μm): the absorbance at 560 nm was completely abolished (~0.01 μA). Variation of the pH (from 1 to 14) or addition of a co-solvent such as dioxane, tetrahydrofurane (THF), dimethylsulfoxide (DMSO), acetone, ethyl acetate, dimethylformamide (DMF), acetonitrile (ACN), methanol (MeOH), ethanol (EtOH) did not completely dissolve the precipitated formazan, even after a 100-fold dilution of the reaction mixture (Fig. 2A).

The bis-tetrazolium salts, such as NBT, have another disadvantage: they can be only partly reduced, resulting in a mixture of mono- and double-reduced formazan products. We therefore selected another tetrazolium salt, this time in the mono-tetrazolium series. Among the commercially available salts used for viability studies (XTT, MTT, MTS, CTC, *etc.*),[31] we selected MTT (Fig. 1B), which has an absorption range different than that of the flavins. Although still precipitating at the end of the reaction, contrarily to NBT-formazan, MTT-formazan was soluble in a wide variety of tested solvents: DMSO, ACN, DMF or THF. We selected THF for dissolving the generated formazan: the reaction mixture was diluted with an equivalent volume of THF and its absorbance at 560 nm before and after filtration on a 0.2 μm syringe filter was identical: A_{560nm} (before) = 0.825; A_{560nm} (after) = 0.814.

Accordingly, MTT was selected as probe to monitor the photosensitizer activity, and THF as co-solvent to dissolve the MTT-formazan generated at the end of the reaction.

b Choice of the flavin's concentration. The reaction conditions should be calibrated in order to allow the ranking of the new flavin photosensitizers compared to the riboflavin. Because this structure-photosensitizing activity is based on the color intensity of the dye, we targeted an absorbance of the colorant in the 0.3–0.4 range. A more active photosensitizer would translate into a higher concentration of the resultant dye (thus its higher absorbance), while a less active photosensitizer would conduct to a lower concentration of the dye. The targeted absorbance of 0.4 would allow, in a first instance, to identify a 3-fold variation of the photosensitizing activity compared to the reference riboflavin without dilution of the reaction medium.

A calibration curve was generated using the commercially-available MTT-formazan (ESI – F1†), and it showed that the concentration necessary to induce an absorbance of 0.4 is 1.275×10^{-4} M. As the reaction between the RF and MTT is stoichiometric, the concentration of RF should be the same. This did not cause any issues, as the aqueous solubility of riboflavin is ~100 mg L^{-1} (~2.66×10^{-4} M).[32]

c Choice of the irradiation source. Riboflavin absorbs light in the UV range at 221, 264, 371 nm, and in the visible range at 443 nm. The source of irradiation should thus emit either in the UV or in the visible range, however, because of the cellular toxicity of the UV light, we shifted to blue light sources, as they are less toxic (or life-compatible). Several in-house blue LED (light emitting diodes) sources were tested allowing to variate the irradiating power to achieve the targeted absorbance of 0.4 reminded above: (a) 1 W (mono-LED, A160 WE Tuna, Kessil; P = 1 W); (b) 5 × 3.3 mW (5 LED, SMD 3528 LED type, P = 3.3 mW); (c) a variable power mono-LED source ranging from 0.7 to 32.5 mW (M455F3 Thorlabs). As shown in Table 1, after 3 minutes of irradiation, the most powerful LED (1 W) delivered a lower MTT-formazan yield (48%) than the less power LEDs (80% and 85%, respectively). This lower yield of MTT-formazan was confirmed to be the result of the flavin's degradation under the intense irradiation conditions (*vide infra*). Finally, an irradiation power

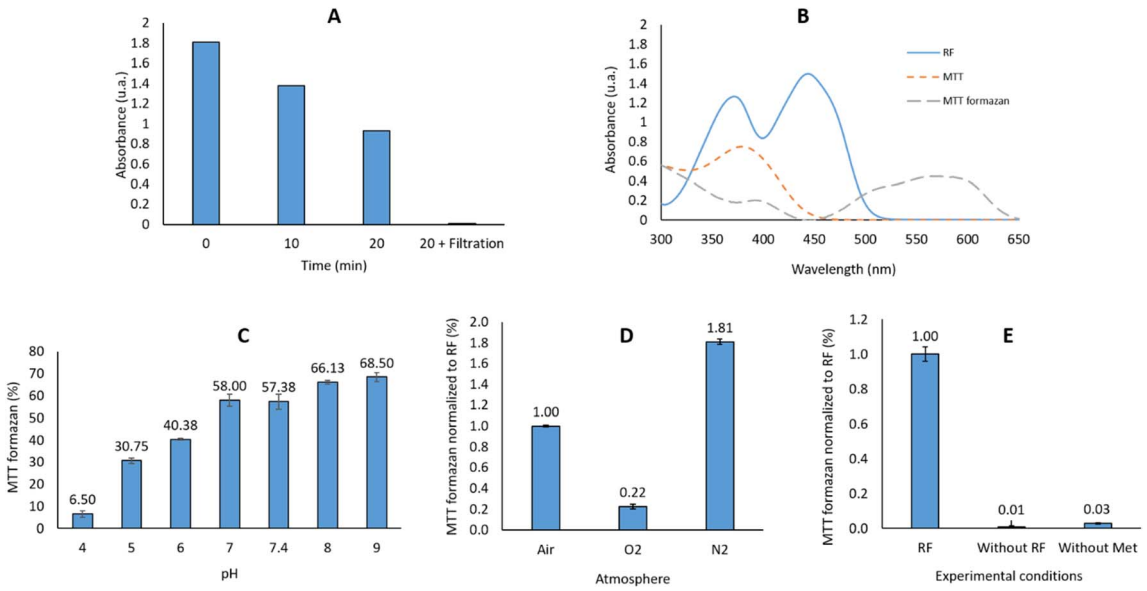

Fig. 2 (A) Absorbance at 560 nm after 0, 10 & 20 min of pause, and after filtration on 0.2 μm filters; (B) UV-Vis spectra of RF (12.8 mM in water), MTT (10.9 mM in water) and MTT-formazan (2.19 mM in THF/water 1/1); (C) influence of the pH on the reaction output; (D) influence of the atmosphere on the reaction output; (E) control reactions: without RF or without methionine.

Table 1 Tested irradiation light sources (irradiation time 3 min)

Power	Light source	$\lambda_{irradiation}$ (nm)	MTT formazan (%)
Without irradiation		—	0
1 W	LED[a]	455	48
5 × 3.3 mW	5 × LED device[b]	460	80
32.5 mW	LED[c]	455	85
6.69 mW	LED[c]	455	40

[a] A160 WE Tuna blue, Kessil, Taiwan. [b] SMD 3528, SignComplex. [c] M455F3, Thorlabs.

of 6.69 mW delivered the targeted 40% of MTT-formazan. It should be noted that no degradation of RF was observed under these conditions. Accordingly, this irradiating power was selected for the other parameters investigations.

In conclusion, the selected light source was the Thorlabs monochromatic M455F3 LED (λ_{em} = 455 nm), modulated by a cube driver (LEDD1B) to an output of 6.69 mW, equipped with the 0.4 mm optical fiber M28L01. This source allowed to attain an Abs = 0.4 for the resultant MTT-formazan after 3 minutes of irradiation of the reaction mixture.

d Choice of the pH. The influence of pH on the sensitization reaction was monitored by adding a basic (NaOH 0.1 N) or acidic solution (HCl 0.1 N) to the reaction mixture. The investigated pH range was between 4 and 9. Fig. 2C shows that, after 3 minutes of irradiation, the reaction seems considerably favored in a basic (pH > 8) *versus* an acidic medium (pH < 5). Contrary to FAD and FMN which have their photosensitizing activities highly dependent on their conformations (extended *vs.* bended),[33] riboflavin's photosensitizing activity is mainly driven by the redox and acid–basic equilibria of the isoalloxazine core (see seminal review of Heelis).[34] In our case, a higher reaction yield as the pH increases could be the result of: (1) an increased MTT-formazan absorbance at higher pH as reported earlier,[35] or (2) of the pH-dependent quantum yield of the photogenerated ^{3}RF*. Plumb *et al.* reported earlier that the absorbance of MTT formazan increases in the pH range 3.5–11.5 in a DMSO or DMSO/glycine buffer solution. As our solvent mixture is different, we investigated if the absorbance dependence reported earlier is similar for the THF/H_2O mixture used for our reaction. As shown in ESI – F2,† the absorbance of commercially available MTT formazan is constant in the 3–12 pH range in the THF/H_2O 1 : 1 mixture used in the reaction. The reaction output in our case is thus dependent on the RF activity at different pH. Our results can be correlated with the previously data on ^{3}RF* quenching in water in a pH dependent manner: Huvaere[36] reported that at a pH = 4.2 the bimolecular rate constant is $k = 4.9 \times 10^7$ L mol^{-1} s^{-1} while at pH = 7 the rate constant is $k = 2.2 \times 10^7$ L mol^{-1} s^{-1}. The initial mechanism described by Huvaere for the interaction of ^{3}RF* and methionine, with the final formation of DMDS (dimethyldisulfide) was questioned later by Bassani *et al.*[37] which proposed another mechanistic pathway for the formation of this odor-repellent product. For a potential usage in the PDT, we decided to use a pH = 6, in order to mimic the slightly acidic tumoral microenvironment. Moreover, this pH allows generation of the 40% reaction output as initially targeted (*vide supra*), necessary to rank different flavins based on this method. It should be reminded that the addition of THF as co-solvent was mandatory for dissolving the generated MTT formazan.

e Influence of the atmosphere. Different reaction atmospheres were also evaluated during our study. In order to saturate the reaction medium with a specific atmosphere, 10 cycles of vacuum/gas bubbling were conducted over 10 min. As shown in Fig. 2D the reaction output is 4.5-fold lower in an O_2-rich medium compared to an air-medium. On the contrary, the reaction output is 1.8-fold higher in a N_2-rich medium. These results can be explained based on the reactivities of the generated radical species.

After excitation by light to the singlet state, subsequently generating the triplet state, ^{3}RF* is reduced by the electron donor present in the reaction (methionine) to the radical anion state RF$^{\bullet -}$.[37–39] This last will trap a proton (H^+) and will subsequently generate the semiquinone RFH$^\bullet$ able to reduce MTT to the corresponding MTT formazan. However, this reaction pattern is modified by the presence of a high concentration of O_2:[38,40] under an O_2-rich medium, the ^{3}RF* quenching by methionine ($k = 6.36 \times 10^7$ M^{-1} s^{-1})[41] is highly overpassed by ^{3}RF* quenching by the O_2 (k = 0.5–1.7 × 10^9 M^{-1} s^{-1}).[38] This last reaction will generate $^1O_2$, which is quenched by the presence of a high excess of methionine in the reaction medium (55 eq. *vs.* 1 eq. MTT/1.1 eq. RF) to a rate previously reported in the range 1.3–1.7 × 10^7 M^{-1} s^{-1}.[42,43] The final result of such a cascade will be a lower amount of the resultant MTT formazan than in an air-saturated solution.

In an N_2-rich medium: a lower concentration of $^1O_2$ will be generated, thus the probability for the ^{3}RF* to be quenched by $^1O_2$ is decreased. The electron transfer from methionine will thus be favored in such an N_2-rich compared to an O_2-rich medium. No reaction takes place in the absence of methionine (*vide infra*).

An air-saturated solution will combine both reactions described before: 20% of O_2 in air will penalize the reaction output compared to N_2-saturated solution (Fig. 2D).

f Control reactions & typical irradiation protocol. The importance of the photosensitizer or of the methionine for the success of the reaction was subsequently verified. As shown in Fig. 2E, in the absence of the photosensitizer the reaction did not proceed. Similar results were obtained if methionine was not added to the reaction mixture (see also ESI – F3†). As expected, the photosensitization reaction did not proceed in the absence of irradiation (Table 1).

It should also be reminded that the photophysics of a photosensitization reaction is temperature sensitive, depending on several factors like the thermal stability (*e.g.* deactivation) of the ^{3}PS or $^1O_2$, the temperature-dependent ground-O_2 solubility and diffusion in water, *etc.* For example, Ogilby *et al.* noted that, contrary to the ^{1}FMN which is less sensitive to temperature variation, the rate constant for quenching ^{3}FMN by ground O_2 increases 10 fold upon increasing the temperature from 10 to 43 °C, having as consequence an increased rate of singlet oxygen formation in this

temperature range.[44] The same increasing photosensitization trend with the temperature increase was described for porphyrin-based photosensitizers (*e.g.* see work of Kimel *et al.*).[45]

As the goal of our study was to develop a straightforward methodology that can be used to compare photosensitization abilities for a series of flavins, this method was optimized at room temperature (20 °C). However, even if riboflavin is a thermostable vitamin,[46] different temperatures *will* impact the reaction output (see ESI – F4† for details), presumably *via* the mechanisms reminded above.

Based on the previous experiments, in a typical irradiation protocol (see *Materials and methods*) an aqueous solution of the investigated flavin (1.275×10^{-4} M, 1 eq.) was mixed with methionine (55 eq.) and MTT (1 eq.) and the pH adjusted to 6 by addition of HCl (aq soln 0.1 N). The mixture was subsequently irradiated for 3 minutes by a blue LED ($\lambda_{max} = 455$ nm, 6.69 mW) under air atmosphere. The reaction mixture was subsequently diluted by addition of an equivalent amount of THF and heated for 5 min at 50 °C. The absorbance of the solution was measured at $\lambda = 560$ nm and reported on a calibration curve prepared from commercially available MTT formazan in THF/H_2O 1/1 for concentrations between 0 and 5.34×10^{-5} M ($y = 0.0631x - 0.0152$, $R^2 = 0.991$).

2 Photo-degradation reactions

It is well known that flavins undergo chemical or metabolic degradation products. If the enzymatic metabolites also generate oxidation products of the isoalloxazine ring, the pH-dependent chemical transformations and the photo-degradation involve mostly ribityl side-chain transformations, the main derivatives being the lumichrome (LC), lumiflavin (LF) and formyllumiflavin (FLF).[47–50] In order to assess the possible photo-degradation products generated under the irradiation conditions and their impact on the photosensitizing activity, the same reaction was conducted for an extended period of time using the same LED sources as before. Comparing the reaction mixture with the commercially available LC and LF by thin layer chromatography (TLC) allowed us to qualitatively estimate the output of the reaction. No traces of LC and LF were detected after 3 min irradiation at 6.69 mW with the M455F3 LED. Traces of these derivatives were observed after 3 minutes of irradiation of the riboflavin sample at 32.5 mW; these products became clearly visible after 15 min of reaction. The LC ratio continuously increased over 2 h, until it was the only product of the reaction. The same LC product was obtained only after 3 minutes when the sample was irradiated with the more powerful 1 W LED (Table 2).

The photosensitizing activities of the commercially available LC and LF were subsequently evaluated using the previously described protocol. As shown in Fig. 3A, LF is equipotent with the RF, while the LC is devoid of any photosensitizing activity. However, it is important to note that LC does not present the same UV spectra as the flavins: it does not absorb at 450 nm, but at lower wavelengths: 355 nm and 385 nm. As described previously by Weiss,[51] LC has the same capacity of inter-system crossing as RF ($\Phi_{ISC} = 0.71$ *vs.* $\Phi_{ISC} = 0.67$),[52] but it requires irradiation at 347 nm which is highly mutagenic compared to the 455 nm range. In conclusion, the selected 3 min irradiation with a LED power of 6.69 mW was mild enough not to degrade RF and validated the irradiation conditions. Such a methodology can be used to rank flavins and their derivatives based on their photosensitizing activity.

Table 2 Photodegradation products obtained from riboflavin[a]

Irradiation power (mW)	Irradiation time (min)	LC	LF
6.69	3	—	—
32.5	3	+	+
32.5	15–90	++	+
32.5	120	+++	—
1000	3	+++	—

[a] "—" indicates no presence of cpd as observed by TLC; "+" indicates traces of cpds; "++" moderate intensity of TLC spots and "+++" main compounds by TLC.

We described one such flavin derivative recently: 7-*t*butyl-desoxyriboflavin (*t*BdRF, Fig. 3B). This was conjugated on phospholipid derivatives through a pentyl linker, in order to induce vesicular self-assemblies (*e.g.* liposomes).[19] With this derivative in our library, we were interested in verifying if it would generate the same photo-degradation products as riboflavin. Degradation of riboflavin is described in the literature to be assisted by the C_2–OH of the ribityl chain.[26] In the case of *t*BdRF, this hydroxyl moiety is absent from the *N*-alkyl chain, in consequence, the mechanism of photo-degradation could be different, or could result in other degradation derivatives. In order to investigate this hypothesis, our irradiation protocol with different irradiation sources was employed. However, contrary to LC and LF, the analogues in 7-*t*butyl-isoalloxazine series are not commercially available, thus they were synthesized in-house, by analogy with the previously reported methods.[53]

Briefly, chlorouracil was engaged in a solvent-free reaction with either 4-*t*butyl-aniline or 4-(*t*butyl)-*N*-methylaniline. The substitution products were subsequently submitted to an *N*-oxidation by sodium nitrite in acetic acid. The instable *N*-oxide intermediate was directly reduced by dithiothreitol (DTT) to the corresponding lumiflavin or lumichrome, depending on the substitution on the N-10 (Scheme 1).

The synthesized compounds in 7-*t*Butyl series (***t*BLC** and ***t*BLF**) present the same UV-Vis patterns as LC and LF.

Thus, despite the low hypochromic effect, the ***t*BLF** spectrum overlaps the *t*BdRF (Fig. 3C). Again, as for RF, the ***t*BLC** does not absorb at the same wavelength as ***t*BLF** (400 nm *vs.* 440 nm). It was expected that ***t*BLC** would not induce any photosensitizing activity using the M455F3 LED ($\lambda_{em} = 455$ nm).

With both ***t*BLC** and ***t*BLF** used as controls, we proceeded with the irradiation of *t*BdRF. Interestingly, no traces of ***t*BLC** or ***t*BLF** were observed by TLC after 15 min of irradiation using the 1 W LED. Other minor compounds were generated in the reaction mixture, which became predominant only after full

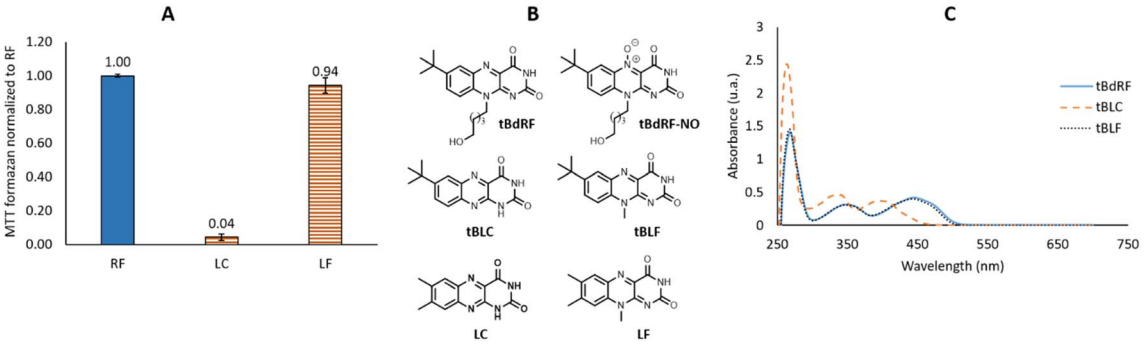

Fig. 3 (A) Photosensitizing activities of RF, LC and LF; (B) chemical structures of *t*BdRF, ***t*BLC**, ***t*BLF**, LC and LF; (C) UV-Vis spectra of *t*BdRF, ***t*BLC** and ***t*BLF**.

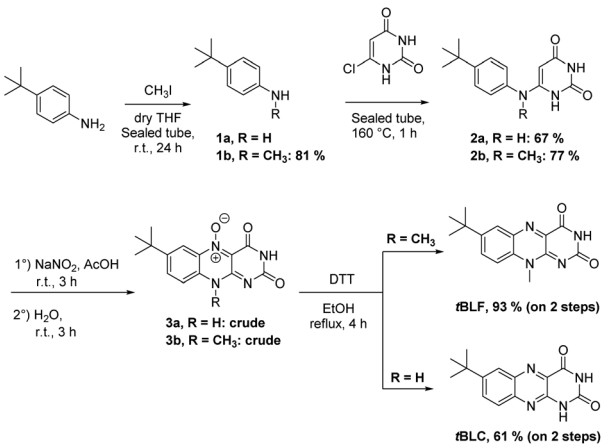

Scheme 1 Synthesis of ***t*BLF** and ***t*BLC**.

consumption of the starting *t*BdRF: after 8 h of reaction. Only traces of the expected ***t*BLC** or ***t*BLF** were observed at the end of the reaction. Unfortunately, the ^{1}H, ^{13}C and MS spectra did not allow identification of the main derivatives generated under these irradiation conditions. From a structural point of view, it is important to underline that no aromatic signals were present in the ^{1}H & ^{13}C spectra of the main photo-degradation products. Hydroxyl moieties present in the structure of RF seem thus to mediate a specific photo-degradation mechanism. In the absence of such –OH moieties, the degradation mechanism was different and led to other derivatives than the corresponding ***t*BLF** and ***t*BLC**. However, in the absence of structural details, no other studies were conducted with these derivatives.

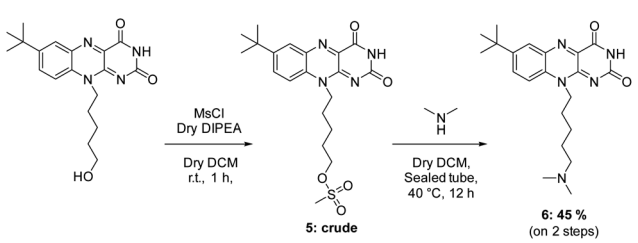

Scheme 2 Synthesis of *t*BdRF-NMe_2.

In all cases, independent of the presence of hydroxyl moieties on the N_{10}-alkyl chain, the selected 3 min irradiation with a LED power of 6.69 mW did not conduct to any photo-degradations. The previously identified irradiation conditions were thus validated.

3 Method validation

Other flavin derivatives were evaluated using this protocol in order to assess its utility for characterizing their photosensitizing abilities. For example, we tested the FMN and other derivatives in the *t*BdRF series belonging to our internal library of flavins. For example, when compared to RF, its biologically active form, FMN, has a 17% lower photosensitizing activity. In order to mimic the micro-tumoral environment, an acidic pH 6 was used during our tests. Under these acidic conditions,[54] FMN can generate the photo-inactive LC. This could explain why its activity is lower than RF. Another derivative of the previously reported *t*BdRF (Fig. 3B) was subsequently investigated: the terminal hydroxyl group was substituted by dimethylamine. This derivative was synthesized after the initial activation of the hydroxyl moiety into a methylsulfonyl (mesylate) leaving group under basic conditions, followed by its substitution by dimethylamine (Scheme 2). Interestingly, using the same irradiation method as before, this derivative has a 51% higher activity than the starting *t*BdRF (Fig. 4). The amine moiety in its structure seems to play a vital role in mediating the protonation state of the isoalloxazine ring, with an impact on the generation of its active triplet state.

A final compound was evaluated for its photosensitizing activity: the *N*-oxide intermediate (Fig. 3B) from our in-house

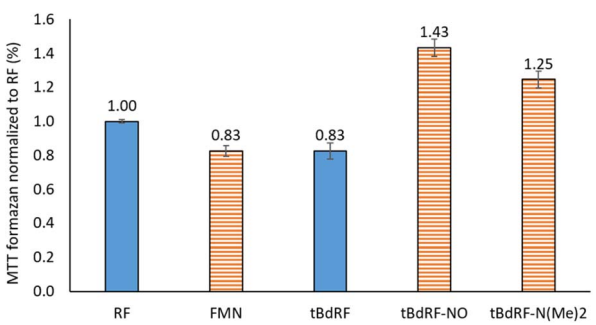

Fig. 4 Photosensitizing activities for a panel of flavins.

library of flavins. Interestingly, the *t*BdRF-NO derivative was found to be 72% more active than the starting *t*BdRF (Fig. 4).

A library of flavin analogues was recently synthesized by our group using a multistep approach. Their photosensitizing activity was evaluated using the methodology reported herein, which allowed identifying lead compounds for potential PDT applications. The best derivative from this series will be conjugated on phospholipids and formulated into liposomes, in order to conduct to a more efficient generation of nano-bombs than those we previously described in the literature.[19] These results will be disclosed in due time.

Conclusion

The current manuscript presents the design of an easy-to-implement protocol used to investigate the photosensitizing activity of flavins. Several parameters were monitored during this study. They were optimized to deliver a 40% reaction output in order to facilitate a direct comparison of the investigated flavins. The retained parameters were: (i) the light source – a blue LED (λ_{em} = 455 nm) at 6.69 mW. A more intense blue LED was observed to induce photo-degradation of the flavins; (ii) the irradiation time – 3 minutes; (iii) the pH – this was adjusted to 6 in order to mimic the tumoral environment; the reaction output was shown to be pH-dependent. For example, compared to a 40% yield at pH = 6, the yields were 7% and 69% at pH = 4 and pH = 9, respectively; (iv) the atmosphere of the reaction medium – the air-saturated medium was found to deliver the optimum reaction rate, intermediate between the O_2- (lower yield) and N_2-saturated reactions (higher yield); (v) the dye to monitor the sensitization efficacy – a tetrazolium derivative (MTT) was used as the precipitated colored MTT-formazan was soluble several organic solvents (THF was selected for dissolving the precipitated MTT-formazan).

The protocol described in the current article is essential for medicinal chemistry projects aiming at identifying potent photosensitizers: the newly synthesized potential photosensitizers should be ranked based on their photosensitizing activities. As a proof of concept, this protocol was used to generate preliminary SAR data for a small panel of compounds. Among them, the *N*-oxide form of a RF analogue was found more photo-active than the parent flavin.

Additionally, a dehydroxylated analogue of riboflavin was found to give photodegradation derivatives other than the expected lumiflavin and lumichrome analogues which were observed for RF. This seems to suggest that, in the absence of an OH group in the C_2 position of the ribityl chain, the mechanism of photo-degradation is different than the one observed for RF.

The method described herein could be used to develop structure–photosensitizing activity relationships for libraries of flavin analogues, with the final goal of identifying potent agents for photo-dynamic therapy.

Experimental

1 Materials and methods

All reagents and solvents were purchased from Sigma-Aldrich, Alfa-Aesar, Acros Organics and were used without further purification. The infrared (IR) spectra were recorded a Jasco FT/IR-4600 spectrometer on a single-reflection diamond ATR accessory. ^{1}H-NMR, ^{13}C-NMR were recorded with Bruker Avance 300 spectrometer (at 300 MHz, 75 MHz) in $CDCl_3$-d_1, CD_3OD-d_4, DMSO-d^6. Chemical shifts are reported in parts per million (ppm) and the coupling constants are reported in units of Hertz [Hz]. Multiplicities were abbreviated as follows: singlet (s), as: apparent singlet, doublet (d), doubled doublet (dd), triplet (t), quintet (quint), multiplet (m). Low resolution mass spectra (MS), were recorded with a Thermo Q Exactive spectrometer. Melting points (Mp) or degradations temperature (T_{deg}) were recorded using a Stuart SMP-30 B-540 apparatus. Flash chromatography was performed on Sigma-Aldrich 52–73 Å (70–230 mesh) silica gel under air pressure. Thin-layer chromatography (TLC) was carried out on Sigma-Aldrich silica gel 60 F254 pre-coated plates. Visualization was made with ultraviolet light (λ = 254/365 nm) or using an aqueous potassium permanganate staining solution.

2 Synthesis

a 4-(*tert*-Butyl)-*N*-methylaniline (1b). Methyl iodide (0.18 mL, 0.40 g, 2.82 mmol, 1 eq.) was added to a solution of 4-*tert*-butylaniline (1.68 g, 11.26 mmol, 4 eq.) in dry THF (10 mL), and the reaction mixture was stirred for 72 h in a sealed tube at room temperature. After the evaporation of solvent, DCM (50 mL) was added. The organic solution was washed with $NaHCO_3$ (aq. satd soln, 20 mL). The organic materials were extracted from the aqueous layer with DCM (3 × 10 mL). The combined organic layers were washed with brine (1 × 5 mL) and dried over $MgSO_4$, filtered and the solvent was evaporated. The residue was purified by flash chromatography on silica gel (PE : EA, 99 : 1 to 9 : 1) to yield compound **1b** as a light brown oil (0.373 g, 81%). $C_{11}H_{17}N$; M = 163.14 g mol^{-1}; IR: ν 3410, 2955 cm^{-1}; MS (ESI): m/z = 148.2 $[M - CH^3]^+$; NMR ^{1}H ($CDCl_3$; 300 MHz): δ (ppm) 1.36 (as, 9H), 2.88 (s, 3H), 3.56 (as, 1H), 6.65 (d, 2H, J = 8.3 Hz), 7.30 (d, 2H, J = 8.6 Hz); NMR ^{13}C ($CDCl_3$; 75 MHz): δ (ppm) 31.0 (CH_3), 31.7 (CH_3), 33.9 (C_q), 112.3 (CH_{ar}), 126.1 (CH_{ar}), 140.2 (C_q), 147.1 (C_q).

b 6-((4-(*tert*-Butyl)phenyl)amino)pyrimidine-2,4(3*H*,5*H*)-dione (2a). 4-*tert*-Butylaniline (0.44 g, 2.70 mmol, 2 eq.) and 6-chlorouracil (0.20 g, 1.35 mmol, 1 eq.) were introduced in a sealed tube. The reaction mixture was stirred for 1 h at 160 °C. The mixture was cooled to room temperature and DCM (20 mL) was added. The residue was subsequently filtrated and washed with DCM (2 × 10 mL) and Et_2O (2 × 10 mL) to yield compound **2a** as a yellow powder (0.350 g, 67%). $C_{14}H_{17}N_3O_2$; M = 259.31 g mol^{-1}; T_{deg} = 353 °C, IR: ν 3235, 2961, 1724, 1600 cm^{-1}; MS (ESI): m/z = 260.1 $[M + H]^+$, 282.1 $[M + Na]^+$; NMR ^{1}H (DMSO-d_6; 300 MHz): δ (ppm) 1.27 (s, 9H), 4.63 (s, 1H), 7.12 (d, 2H, J = 8.6 Hz), 7.40 (d, 2H, J = 8.6 Hz), 8.19 (s, H), 10.11 (s, 1H), 10.42 (s, 1H); NMR ^{13}C (DMSO-d_6; 75 MHz): δ (ppm) (DMSO-d_6; 75 MHz): δ (ppm) 31.1 (CH_3), 34.2 (C_q), 75.4 (CH), 122.7 (CH_{ar}), 126.1 (CH_{ar}), 135.2 (C_q), 147.3 (C_q), 150.8 (C_q), 152.4 (C_q), 164.4 (C_q).

c 6-((4-(*tert*-Butyl)phenyl)(methyl)amino)pyrimidine-2,4(1*H*,3*H*)-dione (2b). Compound **1b** (0.16 g, 0.98 mmol, 2 eq.) and 6-chlorouracil (0.072 g, 0.49 mmol, 1 eq.) were introduced

in a sealed tube. The reaction mixture was stirred for 1 h at 160 °C. The residue was purified by flash-chromatography on silica gel (DCM : MeOH, 100 : 0 to 97 : 3) to yield compound **2b** as a yellow powder (0.103 g, 77%). $C_{15}H_{19}N_3O_2$; M = 273.34 g mol^{-1}; T_{deg} = 290 °C, IR: ν 3416, 2962, 1728, 1624 cm^{-1}; MS (ESI): m/z = 274.1 $[M + H]^+$, 296.1 $[M + Na]^+$; NMR ^{1}H (DMSO-d_6; 300 MHz): δ (ppm) 1.30 (s, 9H), 3.22 (s, 3H), 4.22 (s, 1H), 7.17 (d, 2H, J = 8.3 Hz), 7.45 (d, 2H, J = 8.4 Hz), 10.23 (s, 1H), 10.43 (s, 1H); NMR ^{13}C (DMSO-d_6; 75 MHz): δ (ppm) 31.1 (CH_3), 34.4 (C_q), 39.6 (CH_3), 78.0 (CH), 126.1 (CH_{ar}), 126.6 (CH_{ar}), 141.5 (C_q), 149.5 (C_q), 151.3 (C_q), 155.1 (C_q), 163.7 (C_q).

d 7-(*tert*-Butyl)-benzo[*g*]pteridine-2,4(3*H*,10*H*)-dione (*t*BLC). Sodium nitrite (0.30 g, 4.34 mmol, 5 eq.) was added to a solution of compound **2a** (0.23 g, 0.87 mmol, 1 eq.) in acetic acid (5 mL). After 3 h of stirring at room temperature under nitrogen atmosphere and protected from light with an aluminium foil, water (1.8 mL) was added to the mixture. The obtained suspension was stirred for 3 additional hours. Subsequently, toluene (3 × 10 mL) was added and solvents were co-evaporated. The obtained corresponding *N*-oxide **3a** (orange powder) was then used for the next step as crude (MS (ESI): m/z = 287.1 $[M + H]^+$, 309.0 $[M + Na]^+$). An aqueous solution of DTT (0.61 g, 3.92 mmol, 4.5 eq.), in H_2O (1 mL) was added to a suspension of the crude *N*-oxide **3a** (0.25 g, 0.87 mmol, 1 eq.) in EtOH (22 mL). The mixture was protected from light and refluxed under nitrogen for 4 h. The organic solvent was evaporated and then the residue was filtrated and washed with DCM (3 × 5 mL), H_2O (2 mL) and Et_2O (2 × 5 mL) to conduct to mixture of isomers as a yellow powder (0.235 g, 61% after two steps). $C_{14}H_{14}N_4O_2$; M = 270.29 g mol^{-1}; T_{deg} = 350 °C, IR: ν 3457, 3205, 3085, 1730, 1684 cm^{-1}; MS (ESI): m/z = 293.1 $[M + Na]^+$; NMR ^{1}H (DMSO-d_6; 300 MHz): δ (ppm) 1.37 and 1.41 (s, 9H), 7.76 and 7.85 (d, 1H, J = 8.8 Hz), 7.99 and 8.05 (dd, 1H, J = 2.0 Hz and J = 8.9 Hz), 8.01 and 8.20 (d, 1H, J = 1.9 Hz); NMR ^{13}C (DMSO-d_6; 75 MHz): δ (ppm) 30.6 and 30.7 (CH_3), 34.8 and 35.0 (C_q), 113.7 (CH_{ar}), 121.5 (C_q), 124.8 (CH_{ar}), 126.5 (CH_{ar}), 127.6 (CH_{ar}), 131.4 (C_q), 132.3 (CH_{ar}), 132.4 (CH_{ar}), 135.1 (C_q), 139.0 (C_q), 141.2 (C_q), 142.5 (C_q), 147.3 (C_q), 150.4 (C_q), 150.6 (C_q), 150.9 (C_q), 156.8 (C_q), 160.8 (C_q).

e 7-(*tert*-Butyl)-10-methylbenzo[*g*]pteridine-2,4(3*H*,10*H*)-dione (*t*BLF). Sodium nitrite (0.47 g, 6.77 mmol, 5 eq.) was added to a solution of compound **2b** (0.37 g, 1.35 mmol, 1 eq.) in acetic acid (8 mL). After 3 h of stirring at room temperature under nitrogen atmosphere and protected from light with an aluminium foil, water (2.8 mL) was added to the mixture. The obtained suspension was stirred for 3 additional hours. Subsequently, toluene (3 × 10 mL) was added and solvents were co-evaporated. The obtained corresponding *N*-oxide **3b** (orange powder) was then used for the next step as crude (MS (ESI): m/z = 301.1 $[M + H]^+$, 323.1 $[M + Na]^+$). An aqueous solution of DTT (0.94 g, 6.08 mmol, 4.5 eq.), in H_2O (1.4 mL) was added to a suspension of the crude *N*-oxide **3b** (0.405 g, 1.35 mmol, 1 eq.) in EtOH (34 mL). The mixture was protected from light and refluxed under nitrogen for 4 h. The solvents were evaporated and the residue was purified by flash chromatography on silica gel (PE : EA, 4.6 to EA : MeOH, 95 : 5) to yield compound ***t*BLF** as a yellow powder (0.383 g, 93% after two steps). $C_{15}H_{16}N_4O_2$; M = 284.32 g mol^{-1}; T_{deg} = 319 °C, IR: ν 3446, 2960, 1712, 1679 cm^{-1}; MS (ESI): m/z = 307.1 $[M + Na]^+$; NMR ^{1}H (DMSO-d_6; 300 MHz): δ (ppm) 1.38 (s, 9H), 3.97 (s, 3H), 7.88 (d, 1H, J = 8.8 Hz), 8.05 (m, 2H), 11.39 (s, 1H); NMR ^{13}C (DMSO-d_6; 75 MHz): δ (ppm) 30.8 (CH_3), 31.9 (CH_3), 34.5 (C_q), 116.4 (CH_{ar}), 127.2 (CH_{ar}), 131.3 (C_q), 133.4 (CH_{ar}), 134.6 (C_q), 138.4 (C_q), 149.0 (C_q), 150.7 (C_q), 155.6 (C_q), 159.9 (C_q).

f 7-(*tert*-Butyl)-10-(5-(dimethylamino)pentyl)benzo[*g*]pteridine-2,4(3*H*,10*H*)-dione (6). Mesyl chloride (0.11 mL, 1.40 mmol, 1.25 eq.) was added to a solution of *t*BdRF (0.40 g, 1.12 mmol, 1 eq.) and dry DIPEA (0.29 mL, 1.68 mmol, 1.5 eq.) in dry DCM (10.8 mL). The mixture was stirred for 1 h at room temperature and H_2O (5 mL) was added. The organic materials were extracted from the aqueous layer with DCM (3 × 10 mL). The combined organic layers were dried over $MgSO_4$, filtered and the solvent was evaporated. The residue was used as crude for the next step. Dimethylamine (soln 2 M in THF, 5.6 mL, 11.2 mmol, 10 eq.) was added in sealed tube to the crude **5** (0.48 g, 1.12 mmol, 1 eq.) in dry DCM (5.6 mL). The mixture was stirred for 24 h at 40 °C and $NaHCO_3$ (10% aq. soln 20 mL) was added. The organic materials were extracted from the aqueous layer with DCM (3 × 10 mL). The combined organic layers were dried over $MgSO_4$ filtered and the solvent was evaporated. The residue was purified by flash chromatography on silica gel (DCM : MeOH, 97 : 3 to 9 : 1) to yield compound **6** as a dark orange powder (0.429 g, 45% after two steps). $C_{21}H_{29}N_5O_2$; M = 383.50 g mol^{-1}; Mp = 175 °C, IR: ν 1659, 1243 cm^{-1}; MS (ESI): m/z = 384.24 $[M + H]^+$; NMR ^{1}H (CD_3OD; 300 MHz): δ (ppm) 1.44 (s, 9H), 1.54–1.67 (m, 4H), 1.90 (quint, 2H, J = 7.5 Hz), 2.28 (s, 6H), 2.40 (t, 2H, J = 7.5 Hz), 4.74 (t, 2H, J = 7.7 Hz), 7.93 (d, 1H, J = 9.1 Hz), 8.13 (d, 1H, J = 2.3 Hz, J = 9.0 Hz), 8.17 (s, 1H, J = 2.2 Hz); NMR ^{13}C (CD_3OD; 75 MHz): δ (ppm) 25.5 (CH_2), 27.8 (CH_2), 28.1 (CH_2), 31.3 (CH_3), 35.7 (C_q), 45.3 (CH_3), 46.3 (CH_2), 60.3 (CH_2), 117.2 (CH_{ar}), 129.1 (CH_{ar}), 132.2 (C_q), 135.7 (CH_{ar}), 137.2 (C_q), 139.0 (C_q), 151.7 (C_q), 151.7 (C_q), 159.1 (C_q), 162.3 (C_q).

3 Photosensitizing activity

Stock aqueous solutions of riboflavin (1.275 × 10^{-4} M, pH 6.0), synthesized isoalloxazine derivatives (1.275 × 10^{-4} M, pH 6.0), thiazolyl blue tetrazolium bromide (MTT, 9.65 × 10^{-4} M), and L-methionine (5.66 × 10^{-2} M) were freshly prepared using ultrapure water before the experiments. Flavins (aq. soln, 2.66 mL, 3.39 × 10^{-4} mmol) were mixed with 0.34 mL of the second solution (MTT, 3.28 × 10^{-4} mmol; and L-methionine, 1.52 × 10^{-2} mmol) in a standard test tube (NAFVSM 621.1225075080.9R000) under air atmosphere.

The reaction mixtures were irradiated by direct contact between the reaction vial and a blue LED (λ_{em} = 455 nm) at 6.69 mW (M455F3 LED, optical fiber M28L01 0.4 mm and cube driver LEDD1B were purchased from Thorlabs). The output light intensity was measured at a distance of 0.2 cm using the Thorlab PM400 Console and a S120VC probe prior to irradiation experiments. The reaction mixture was irradiated for 3 min. The generated suspension of MTT formazan was dissolved by adding THF (3 mL) and subsequently heated for 5 min at 50 °C. Its absorbance was measured at λ = 560 nm and reported to

a calibration curve prepared with commercial MTT formazan in THF/H_2O (1/1) for concentrations between 0 and 5.34×10^{-5} M ($y = 0.0631x - 0.0152$, $R^2 = 0.9991$). The experimental setup is described in ESI – F5.†

Abbreviations

DCM	Dichloromethane
DIPEA	Diisopropylethylamine
DTT	Dithiotreitol
EA	Ethyl acetate
PE	Petroleum ether
aq. sat. soln	Saturated aqueous solution
MeOH	Methanol
TEA	Triethylamine
THF	Tetrahydrofurane
RF	Riboflavin
*t*BdRF	*tert*-Butyl desoxyriboflavin
C_{ar}	Aromatic carbon
C_q	Quaternary carbon
ESI	Electrospray ionization
PTFE	Polytetrafluoroethylene
THF	Tetrahydrofurane
DMSO	Dimethylsulfoxide
DMF	Dimethylformamide
ACN	Acetonitrile
MeOH	Methanol
EtOH	Ethanol
NBT	Nitro-blue-tetrazolium
XTT	2,3-Bis-(2-methoxy-4-nitro-5-sulfophenyl)-2*H*-tetrazolium-5-carboxanilide
MTT	3-(4,5-Dimethylthiazol-2-yl)-2,5-diphenyltetrazolium bromide
MTS	3-(4,5-Dimethylthiazol-2-yl)-5-(3-carboxymethoxyphenyl)-2-(4-sulfophenyl)-2*H*-tetrazolium
CTC	5-Cyano-2,3-ditolyl tetrazolium chloride
LED	Light emitting diode
PDT	Photo dynamic therapy
ROS	Reactive oxygenated species
LC	Lumichrome
LF	Lumiflavin
FLF	Formyllumiflavin
TLC	Thin layer chromatography
DTT	Dithiothreitol
TEMPO	(2,2,6,6-Tetramethyl-piperidin-1-yl)oxyl

Conflicts of interest

There are no conflicts to declare.

Acknowledgements

This project was financially supported by the "Ligue Contre le Cancer" Foundation (Nano-Bombs/2019 to EB). The support of the technical platforms of CBMN for the characterization of the new compounds is also acknowledged.

References

1 *IUPAC – Compendium of Chemical Terminology (Gold Book)*, **https://goldbook.iupac.org**.
2 X. Zhao, J. Liu, J. Fan, H. Chao and X. Peng, *Chem. Soc. Rev.*, 2021, **50**, 4185–4219.
3 T. C. Pham, V.-N. Nguyen, Y. Choi, S. Lee and J. Yoon, *Chem. Rev.*, 2021, **121**, 13454–13619.
4 T. Hu, Z. Wang, W. Shen, R. Liang, D. Yan and M. Wei, *Theranostics*, 2021, **11**, 3278–3300.
5 Q. Xiao, J. Wu, X. Pang, Y. Jiang, P. Wang, W. A. Leung, L. Gao, S. Jiang and C. Xu, *Curr. Med. Chem.*, 2018, **25**, 839–860.
6 N. A. Romero and D. A. Nicewicz, *Chem. Rev.*, 2016, **116**, 10075–10166.
7 T. Nyokong and V. Ahsen, *Photosensitizers in Medicine, Environment, and Security*, Springer Science & Business Media, Berlin, Germany, 2012, ISBN 978-90-481-3870-8.
8 A. S. Dunn, *Polym. Int.*, 1998, **45**, 240.
9 J.-H. Shon and T. S. Teets, *ACS Energy Lett.*, 2019, **4**, 558–566.
10 C.-F. Leung and T.-C. Lau, *Energy Fuels*, 2021, **35**, 18888–18899.
11 E. Sassetti, M. H. Clausen and L. Laraia, *J. Med. Chem.*, 2021, **64**, 5252–5275.
12 D. P. S. O'Brart, *J. Optom.*, 2014, **7**, 113–124.
13 F. Raiskup, A. Theuring, L. E. Pillunat and E. Spoerl, *J. Cataract Refractive Surg.*, 2015, **41**, 41–46.
14 B. G. Solheim, *Transfus. Apheresis Sci.*, 2008, **39**, 75–82.
15 S. Marschner, L. D. Fast, W. M. Baldwin III, S. J. Slichter and R. P. Goodrich, *Transfusion*, 2010, **50**, 2489–2498.
16 L. D. Fast, M. Nevola, J. Tavares, H. L. Reddy, R. P. Goodrich and S. Marschner, *Transfusion*, 2013, **53**, 373–381.
17 F. Marlin, P. Simon, S. Bonneau, P. Alberti, C. Cordier, C. Boix, L. Perrouault, A. Fossey, T. Saison-Behmoaras, M. Fontecave and C. Giovannangeli, *ChemBioChem*, 2012, **13**, 2593–2598.
18 T. Komatsu, M. Moritake, A. Nakagawa and E. Tsuchida, *Chem.–Eur. J.*, 2002, **8**, 5469–5480.
19 J. Ribes, N. Beztsinna, R. Bailly, S. Castano, E. Rascol, N. Taib-Maamar, E. Badarau and I. Bestel, *Bioconjugate Chem.*, 2021, **32**, 553–562.
20 D. E. J. G. J. Dolmans, D. Fukumura and R. K. Jain, *Nat. Rev. Cancer*, 2003, **3**, 380–387.
21 M. S. Baptista, J. Cadet, P. Di Mascio, A. A. Ghogare, A. Greer, M. R. Hamblin, C. Lorente, S. C. Nunez, M. S. Ribeiro, A. H. Thomas, M. Vignoni and T. M. Yoshimura, *Photochem. Photobiol.*, 2017, **93**, 912–919.
22 C. Lu, W. Lin, W. Wang, Z. Han, S. Yao and N. Lin, *Phys. Chem. Chem. Phys.*, 2000, **2**, 329–334.
23 Y.-T. Kao, C. Saxena, T.-F. He, L. Guo, L. Wang, A. Sancar and D. Zhong, *J. Am. Chem. Soc.*, 2008, **130**, 13132–13139.
24 M. Insińska-Rak and M. Sikorski, *Chem.–Eur. J.*, 2014, **20**, 15280–15291.

25 K. Sztandera, M. Gorzkiewicz and B. Klajnert-Maculewicz, *Wiley Interdiscip. Rev.: Nanomed. Nanobiotechnol.*, 2020, **12**, e1509.
26 D. Cardoso, S. Libardi and L. Skibsted, *Food Funct.*, 2012, **3**, 487–502.
27 C. B. Martin, M.-L. Tsao, C. M. Hadad and M. S. Platz, *J. Am. Chem. Soc.*, 2002, **124**, 7226–7234.
28 Y. Nosaka and A. Y. Nosaka, *Chem. Rev.*, 2017, **117**, 11302–11336.
29 Y. Zhang, M. Dai and Z. Yuan, *Anal. Methods*, 2018, **10**, 4625–4638.
30 J.-Y. Liang, J.-M. P. Yuann, Z.-J. Hsie, S.-T. Huang and C.-C. Chen, *J. Photochem. Photobiol., B*, 2017, **174**, 355–363.
31 J. C. Stockert, R. W. Horobin, L. L. Colombo and A. Blázquez-Castro, *Acta Histochem.*, 2018, **120**, 159–167.
32 Pubchem, *RF*, **https://pubchem.ncbi.nlm.nih.gov/compound/493570**, accessed 2022-06-01.
33 A. Sengupta, R. V. Khade and P. Hazra, *J. Photochem. Photobiol., A*, 2011, **221**, 105–112.
34 P. F. Heelis, *Chem. Soc. Rev.*, 1982, **11**, 15–39.
35 J. A. Plumb, R. Milroy and S. B. Kaye, *Cancer Res.*, 1989, **49**, 4435–4440.
36 K. Huvaere, M. L. Andersen, M. Storme, J. Van Bocxlaer, L. H. Skibsted and D. De Keukeleire, *Photochem. Photobiol. Sci.*, 2006, **5**, 961–969.
37 A. Furet, A. Sicello, B. Guillemat, C. Absalon, E. Langleron and D. M. Bassani, *Food Chem.*, 2022, **372**, 131281.
38 H. Görner, *J. Photochem. Photobiol., B*, 2007, **87**, 73–80.
39 P. Mondal, K. Schwinn and M. Huix-Rotllant, *J. Photochem. Photobiol., A*, 2020, **387**, 112164.
40 L. Valle, F. E. M. Vieyra and C. D. Borsarelli, *J. Phys. Org. Chem.*, 2016, **29**, 629–635.
41 D. R. Cardoso, D. W. Franco, K. Olsen, M. L. Andersen and L. H. Skibsted, *J. Agric. Food Chem.*, 2004, **52**, 6602–6606.
42 A. Michaeli and J. Feitelson, *Photochem. Photobiol.*, 1994, **59**, 284–289.
43 I. B. C. Matheson and J. Lee, *Photochem. Photobiol.*, 1979, **29**, 879–881.
44 M. Westberg, M. Bregnhøj, M. Etzerodt and P. R. Ogilby, *J. Phys. Chem. B*, 2017, **121**, 2561–2574.
45 V. Gottfried and S. Kimel, *J. Photochem. Photobiol., B*, 1991, **8**, 419–430.
46 E. Choe, R. Huang and D. B. Min, *J. Food Sci.*, 2005, **70**, R28–R36.
47 W. Holzer, J. Shirdel, P. Zirak, A. Penzkofer, P. Hegemann, R. Deutzmann and E. Hochmuth, *Chem. Phys.*, 2005, **308**, 69–78.
48 G. E. Treadwell, W. L. Cairns and D. E. Metzler, *J. Chromatogr. A*, 1968, **35**, 376–388.
49 W. M. Moore, J. T. Spence, F. A. Raymond and S. D. Colson, *J. Am. Chem. Soc.*, 1963, **85**, 3367–3372.
50 P. Hemmerich, C. Veeger and H. C. S. Wood, *Angew. Chem., Int. Ed.*, 1965, **4**, 671–687.
51 M. S. Grodowski, B. Veyret and K. Weiss, *Photochem. Photobiol.*, 1977, **26**, 341–352.
52 W. Moore, J. McDaniels and J. Hen, *Photochem. Photobiol.*, 1977, **25**, 505–512.
53 S.-Y. Ju and F. Papadimitrakopoulos, *J. Am. Chem. Soc.*, 2008, **130**, 655–664.
54 S. L. J. Tan, J. M. Kan and R. D. Webster, *J. Phys. Chem. B*, 2013, **117**, 13755–13766.